PERGAMON

International Journal of Solids and Structures 40 (2003) 3069–3088

INTERNATIONAL JOURNAL OF SOLIDS and STRUCTURES

www.elsevier.com/locate/ijsolstr

Free vibrations of multilayered doubly curved shells based on a mixed variational approach and global piecewise-smooth functions

Arcangelo Messina *

Dipartimento di Ingegneria dell'Innovazione, Università di Lecce, Via Monteroni, 73100 Lecce, Italy

Received 31 May 2002; accepted 3 February 2003

Abstract

This paper presents the extension of a two-dimensional model that, recently appeared in literature, deals with freely vibrating laminated plates. The extension takes into account the corresponding theory describing the dynamic of freely vibrating multilayered doubly curved shells. The relevant governing differential equations, associated boundary conditions and constitutive equations are derived from one of Reissner's mixed variational theorems. Both the governing differential equations and the related boundary conditions are presented in terms of resultant stresses and displacements. In spite of the multi-layer nature of the shell, the theory is developed as if the shell were virtually made of a single layer. This choice does not limit the performances of the model, which are comparable to the corresponding three-dimensional theory. This ability is accomplished by an appropriate global expansion of the relevant kinetic and stress quantities, through the thickness of the multilayered shell. The mentioned expansion is realized by a novel selection of global piecewise-smooth functions. Numerical tests illustrate the performance of the model with respect to several elements subjected to a class of simply supported boundary conditions: plates, circular cylindrical shells, spherical and saddle-shape laminates. The model is first tested by comparing its resulting *eigen-parameters*, with those few existing of exact or approximate three-dimensional models and, finally, new results are provided for several geometrical and material characteristics for plates and shells.

Keywords: Free vibrations; Multilayered systems; Doubly curved shells; Mixed variational approaches

1. Introduction

With respect to the classification that can be done for the theories of freely vibrating laminated plates, the relevant theories describing the dynamic behavior of laminated shells are subjected to further complications. The additional complexities introduced by the curvature, even in Love's classical first approximation, can deal with several kinds of sub-theories that contain or neglect different effects (Leissa, 1973).

* Fax: +39-0832-320-279.
E-mail address: arcangelo.messina@unile.it (A. Messina).

0020-7683/03/$ - see front matter © 2003 Elsevier Science Ltd. All rights reserved.
doi:10.1016/S0020-7683(03)00115-X

However, if sub-models are left out of considerations the two-dimensional theories concerned with shells, could be classified in classical shell theories (CST) (Leissa, 1973), uniform shear deformable shell theories (USDST) (Leissa, 1973; Reddy, 1984) and higher-order shear deformable shell theories (HSDST) (Bhimaraddi, 1984; Reddy and Liu, 1985). The three-dimensional theory has also been taken into account for certain classes of boundary conditions, geometries and material arrangements from other investigators (Bhimaraddi, 1991; Fan and Zhang, 1992; Soldatos, 1994; Huang, 1995; Ye and Soldatos, 1994; Wu et al., 1996). These latter works provide numerical results that can be used as benchmarks for the validity of corresponding dynamic analysis of doubly curved shells when approximated two-dimensional theories are used.

As far as the aforementioned two-dimensional theories are concerned it is popularly intended that the acronyms (CST, USDST and HSDST) refer to those models describing in a global sense (through the whole thickness of the laminate) the related assumptions in the frame of the *method of the hypotheses*. However, although these theories are intended in a global sense the same assumption can also be made through the whole thickness of the laminate at a layer-by-layer level. In the first case the continuity requirements (for displacement and related transverse stresses) could be violated (Bhimaraddi, 1984; Reddy and Liu, 1985; Timarci and Soldatos, 1995; Messina and Soldatos, 1999a,b) whilst in the second case the continuity requirements can be imposed at each interface between the bonded layers (Di Sciuva, 1987; Di Sciuva and Carrera, 1992; Soldatos and Timarci, 1993; Timarci and Soldatos, 1995; Xavier et al., 1995) and, therefore, the continuities can be fulfilled. The second case deserves particular attention due to certain recent developments (Messina and Soldatos, 1999a,b, 2002). These works, not only substantiated the need of the continuity requirements but they also showed the importance of further refining certain shape functions which could better fit the actual in-plane displacements and the interested transverse stresses.

The application of a theory at a layer-level and its subsequent expansion at a global level is mainly complicated by the basic assumption of all the aforementioned two-dimensional theories: they are displacement-based theories and consequently after assuming a global displacement field the constitutive equations naturally lead to discontinuous transverse stresses in a multilayered structure. For this reason, algebraic/differential manipulations have to be necessarily introduced into the model to fulfill the appropriate continuity requirements at the interfaces to obtain an appropriate global theory. This can not only yield a complicate displacement-based theory but it also makes the extension to a higher number of degrees of freedom not immediate.

Mixed-based approach could overcome such difficulties because displacements and stresses can be independently assumed. In this respect Carrera (1999a,b) extended the application of Reissner's variational theorem (Reissner, 1986) to corresponding dynamic studies for multilayered shells as well as taking into consideration the effects of the normal stresses. In these works Legendre polynomials up to the fourth-order (LW4 model) were used to describe transverse stresses and displacements within each (say kth) layer. The continuity requirements were explicitly introduced thus yielding a formulation depending on the displacement and stress unknowns for each layer, therefore, making up a model depending on the number of layers. Messina (2001) investigated the possibility of using Reissner's work (1986) to make up a model that could be independent from the complexity of the number of layers involved. In this attempt Messina (2001), did not completely fulfill the continuity requirements. However, the comparisons with other global displacement-based theories suggested a certain superiority of the relevant mixed model (M2D) for dealing with vibrating multilayered plates. Such superiority could be attributed to the more physical fulfillments that the mixed model permitted. After this first test, Messina (2002a) generalized the idea of making up a theory that would separate the mathematical model of a freely vibrating multilayered plate (M3D) from the functional base. Namely, Messina (2002a) introduced a global theory based on Reissner's theorem (1986) that could be adopted with any suitable functional base. Once the theory was introduced, a novel functional base was separately provided. This latter was constituted by global piecewise-smooth functions (GPSFs) that were able to fulfill the external boundary conditions and the interlaminar continuity requirements. An

excellent numerical/computational performance resulted from the conjunction between M3D and the GPSFs. Indeed, the global theory developed by Messina (2002a) was able to contain previous full layerwise theories as well as three-dimensional results were efficiently and stably obtainable for several geometries and material arrangements. The benefits in using GPSFs rather than classical functional bases were also illustrated in Messina (2002b).

This work intends to generalize the previously presented M3D theory (Messina, 2002a) for plates to the case of doubly curved shells. No restriction regarding stresses or displacements is made. The governing equations are obtained in terms of resultant stresses and displacements for monoclinic layers. In order to verify the accuracy of the present model the equations are solved once they are tailored for orthotropic layers of multilayered doubly curved shells with edges subjected to a simply supported boundary condition. The shell is adapted for several geometries (plates, circular cylindrical shells, spherical and saddle-shape laminates) and all the relevant results are compared with those few existing three-dimensional results. The comparisons make clear that the present theory, regardless of its two-dimensional nature, is able to efficiently approach the three-dimensional results for the majority of the two-dimensional elements used in several engineering applications. Therefore, based on the performance shown by these comparisons, new results are provided with respect to certain fiber reinforced materials, which cover a wide area of engineering applications.

2. Theoretical modeling: dynamics of doubly curved shells

Consider a multilayered doubly curved shell (Fig. 1) having a global thickness h measured through the normal $\mathbf{n}$, which, point-by-point, is perpendicular to the reference surface π_{12}. A curvilinear coordinate system, located on the reference surface with respect to its orthogonal lines of principal directions, is also indicated in Fig. 1 $(\mathbf{r}_{,\alpha 1}/|\mathbf{r}_{,\alpha 1}|, \mathbf{r}_{,\alpha 2}/|\mathbf{r}_{,\alpha 2}|, \mathbf{n})$, being $(\,)_{,x} = \partial(\,)/\partial x$. R_1 and R_2 are the constant radii of curvature to the reference surface along the α_1- and α_2-curves, respectively. The fibers-direction can be considered with respect to the α_1-curve and the layers are counted from $z < 0$. The position vector $\mathbf{R}$ of a point P in the shell corresponds to a position vector $\mathbf{r}$ placed on the reference surface as reported in (1).

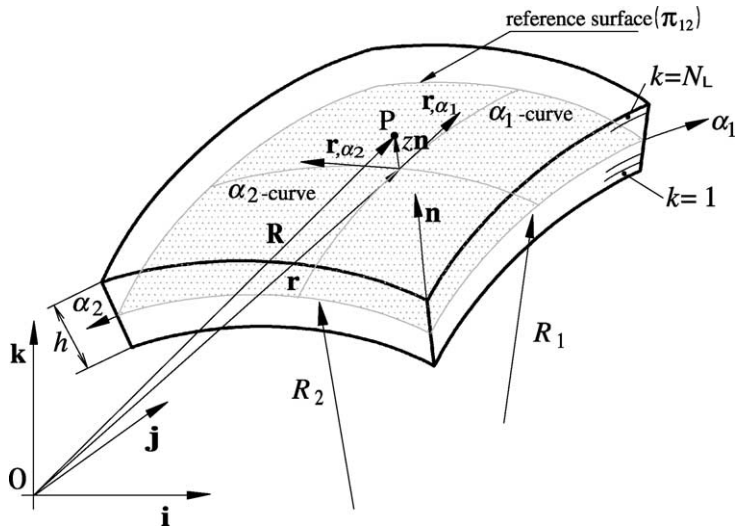

Fig. 1. Nomenclature and coordinate system of the doubly curved laminated shell.

$$\mathbf{R}(\alpha_1,\alpha_2,z)=\mathbf{r}(\alpha_1,\alpha_2)+z\mathbf{n}(\alpha_1,\alpha_2). \tag{1}$$

From Eq. (1) an elementary length in the shell (d Line) (see for example Kraus, 1967; Calcote, 1969) can be expressed through the following equation:

$$\mathrm{d\,Line}^2=A_1^2h_1^2\mathrm{d}\alpha_1^2+A_2^2h_2^2\mathrm{d}\alpha_2^2+\mathrm{d}z^2 \tag{2}$$

being $A_q^2=\mathbf{r}_{,\alpha q}^{o}\,\mathbf{r}_{,\alpha q}$ first fundamental quantities and $h_q=1+z/R_q$. The coordinates elementary surface (d Sur) and volume (d Vol) can be obtained through Eq. (2).

The shell is considered as elastically heterogeneous in the thickness direction with a local symmetry with respect to $\mathbf{n}$. The following form of Hooke's generalized law gives the local stress–strain relation

$$\begin{pmatrix}\sigma_1\\ \sigma_2\\ \sigma_z\\ \tau_{2z}\\ \tau_{1z}\\ \tau_{12}\end{pmatrix}=\begin{bmatrix}C_{11} & C_{12} & C_{13} & 0 & 0 & C_{16}\\ & C_{22} & C_{23} & 0 & 0 & C_{26}\\ & & C_{33} & 0 & 0 & C_{36}\\ & \mathrm{sym} & & C_{44} & C_{45} & 0\\ & & & & C_{55} & 0\\ & & & & & C_{66}\end{bmatrix}\cdot\begin{pmatrix}\varepsilon_1\\ \varepsilon_2\\ \varepsilon_z\\ \gamma_{2z}\\ \gamma_{1z}\\ \gamma_{12}\end{pmatrix}, \tag{3}$$

where $(\sigma_1,\sigma_2,\sigma_z,\tau_{2z},\tau_{1z},\tau_{12})$ and $(\varepsilon_1,\varepsilon_2,\varepsilon_z,\gamma_{2z},\gamma_{1z},\gamma_{12})$ are the stress and strain components respectively. The elastic heterogeneity of the shell through its thickness (h) is established by the elastic constant C_{ij} that are piecewise continuous.

Based on the displacement field of a point $P(\alpha_1,\alpha_2,z)$ through the adopted curvilinear coordinates

$$\mathbf{U}(\alpha_1,\alpha_2,z)=U(\alpha_1,\alpha_2,z)\mathbf{t}_1+V(\alpha_1,\alpha_2,z)\mathbf{t}_2+W(\alpha_1,\alpha_2,z)\mathbf{n}, \tag{4}$$

where $(\mathbf{t}_1,\mathbf{t}_2)$ correspond to tangent unit vectors on the reference surface (i.e. $\mathbf{r}_{,\alpha1}/|\mathbf{r}_{,\alpha1}|,\mathbf{r}_{,\alpha2}/|\mathbf{r}_{,\alpha2}|$), the kinetic relations herein considered ($A_{q,\alpha m}=0$; q, $m=1,2$) are the following:

$$\begin{aligned}&\varepsilon_1=\frac{1}{h_1}\left(\frac{1}{A_1}\cdot\frac{\partial U}{\partial\alpha_1}+\frac{W}{R_1}\right),\quad \varepsilon_2=\frac{1}{h_2}\left(\frac{1}{A_2}\cdot\frac{\partial V}{\partial\alpha_2}+\frac{W}{R_2}\right),\quad \gamma_{12}=\frac{1}{A_1h_1}\cdot\frac{\partial V}{\partial\alpha_1}+\frac{1}{A_2h_2}\cdot\frac{\partial U}{\partial\alpha_2},\\ &\varepsilon_3=\frac{\partial W}{\partial z},\quad \gamma_{2z}=\frac{\partial V}{\partial z}+\frac{1}{h_2}\left(\frac{1}{A_2}\cdot\frac{\partial W}{\partial\alpha_2}-\frac{V}{R_2}\right),\quad \gamma_{1z}=\frac{\partial U}{\partial z}+\frac{1}{h_1}\left(\frac{1}{A_1}\cdot\frac{\partial W}{\partial\alpha_1}-\frac{U}{R_1}\right).\end{aligned} \tag{5}$$

Under these considerations, the present mixed elastic shell model begins with the following displacement and stress assumption:

$$\begin{aligned}&U(\alpha_1,\alpha_2,z;t)=\Phi(z)_{1j}u(\alpha_1,\alpha_2;t)_j,\quad V(\alpha_1,\alpha_2,z;t)=\Phi(z)_{2j}v(\alpha_1,\alpha_2;t)_j,\\ &W(\alpha_1,\alpha_2,z;t)=\Phi(z)_{3j}w(\alpha_1,\alpha_2;t)_j,\end{aligned} \tag{6}$$

$$\begin{aligned}&\tau(\alpha_1,\alpha_2,z;t)_{2z}=\Psi(z)_{1p}\tau(\alpha_1,\alpha_2;t)_{2zp},\quad \tau(\alpha_1,\alpha_2,z;t)_{1z}=\Psi(z)_{2p}\tau(\alpha_1,\alpha_2;t)_{1zp},\\ &\sigma(\alpha_1,\alpha_2,z;t)_z=\Psi(z)_{3p}\sigma(\alpha_1,\alpha_2;t)_{zp},\end{aligned} \tag{7}$$

where in each single equation, (6), (7), as in the following, the indices ($j,p=1,2,\ldots,N_u,N_\sigma$) are assumed to be repeated in place of the relevant summation. Moreover, the approximating global functions $(\Phi(z)_{1i},\Phi(z)_{2i},\Phi(z)_{3i},\ \Psi(z)_{1q},\Psi(z)_{2q},\Psi(z)_{3q})$ defined through the whole thickness of the shell $(-1/2\leqslant z/h=\zeta\leqslant 1/2)$ are intended dimensionless. The two-dimensional displacement and stress components are conversely dimensionally consistent with their counterparts.

The approximating global functions are responsible for fulfilling the boundary conditions on the top and bottom of the plate as well as for satisfying the appropriate interlaminar continuity conditions. Both these

aspects will be further discussed in Section 3. This section is only devoted to develop a global mixed shell theory without mentioning anyone of the mathematical characteristics associated with the approximating global functions. Therefore, the present theory could be conveniently used for any suitable set of global approximating functions, which might or might not be that suggested in Section 3 of this paper (GPSFs).

Once the related assumptions of the stress and displacement (6), (7) are made, the following variational statement (8) (Reissner, 1986), tailored for the dynamic case (Carrera, 1999a,b; Messina, 2001, 2002a), can be used to obtain the governing equations of motion in conjunction with boundary conditions.

$$\int_{\mathrm{Vol}} \boldsymbol{\sigma}_{\mathrm{in}}^{\mathrm{T}} \delta \mathbf{e}_{\mathrm{in}}^{(\mathrm{G})} + \boldsymbol{\sigma}_{\mathrm{ou}}^{\mathrm{T}} \delta \mathbf{e}_{\mathrm{ou}}^{(\mathrm{G})} + \delta \boldsymbol{\sigma}_{\mathrm{ou}}^{\mathrm{T}} \left(\mathbf{e}_{\mathrm{ou}}^{(\mathrm{G})} - \mathbf{e}_{\mathrm{ou}}^{(\mathrm{C})} \right) \mathrm{d}\,\mathrm{Vol} + \int_{\mathrm{Vol}} \rho \left(\ddot{U} \delta U + \ddot{V} \delta V + \ddot{W} \delta W \right) \mathrm{d}\,\mathrm{Vol} = 0. \tag{8}$$

In Eq. (8) the superscript 'T' stands for the transpose operator while the superscripts in parentheses (G, C) state that the relevant strains ($\mathbf{e}_{\mathrm{ou}}^{\mathrm{T}} = (\gamma_{2z}, \gamma_{1z}, \varepsilon_z); \mathbf{e}_{\mathrm{in}}^{\mathrm{T}} = (\varepsilon_1, \varepsilon_2, \gamma_{12})$) should be introduced into Eq. (8) by using the geometric equations (5) and the constitutive equations (3), respectively. Finally, out-of-plane and in-plane stresses ($\boldsymbol{\sigma}_{\mathrm{ou}}^{\mathrm{T}} = (\tau_{2z}, \tau_{1z}, \sigma_z); \boldsymbol{\sigma}_{\mathrm{in}}^{\mathrm{T}} = (\sigma_1, \sigma_2, \tau_{12})$) should be considered through the assumed field equations (7) and the constitutive equations (3), respectively. However, in order to apply the variational statement (8) the constitutive equations (3) should be adopted in the following equivalent form:

$$\begin{Bmatrix} \begin{Bmatrix} \sigma_1 \\ \sigma_2 \\ \tau_{12} \end{Bmatrix} \\ \begin{Bmatrix} \tau_{2z} \\ \tau_{1z} \\ \sigma_z \end{Bmatrix} \end{Bmatrix} = \begin{bmatrix} \begin{bmatrix} C_{11} & C_{12} & C_{16} \\ C_{12} & C_{22} & C_{26} \\ C_{16} & C_{26} & C_{66} \end{bmatrix} & \begin{bmatrix} 0 & 0 & C_{13} \\ 0 & 0 & C_{23} \\ 0 & 0 & C_{36} \end{bmatrix} \\ \begin{bmatrix} 0 & 0 & 0 \\ 0 & 0 & 0 \\ C_{13} & C_{23} & C_{36} \end{bmatrix} & \begin{bmatrix} C_{44} & C_{45} & 0 \\ C_{45} & C_{55} & 0 \\ 0 & 0 & C_{33} \end{bmatrix} \end{bmatrix} \cdot \begin{Bmatrix} \begin{Bmatrix} \varepsilon_1 \\ \varepsilon_2 \\ \gamma_{12} \end{Bmatrix} \\ \begin{Bmatrix} \gamma_{2z} \\ \gamma_{1z} \\ \varepsilon_z \end{Bmatrix} \end{Bmatrix}$$

$$= \begin{bmatrix} \mathbf{C}_{126} & \mathbf{D} \\ \mathbf{D}^{\mathrm{T}} & \mathbf{C}_{345} \end{bmatrix} \begin{Bmatrix} \mathbf{e}_{\mathrm{in}} \\ \mathbf{e}_{\mathrm{ou}} \end{Bmatrix} \tag{9}$$

from which the in-plane stresses and out-of-plane strains can be expressed as follows:

$$\begin{aligned} \boldsymbol{\sigma}_{\mathrm{in}} &= (\mathbf{C}_{126} - \mathbf{D} \cdot \mathbf{C}_{345}^{-1} \mathbf{D}^{\mathrm{T}}) \mathbf{e}_{\mathrm{in}} + \mathbf{D} \cdot \mathbf{C}_{345}^{-1} \boldsymbol{\sigma}_{\mathrm{ou}}, \\ \mathbf{e}_{\mathrm{ou}} &= \mathbf{C}_{345}^{-1} \boldsymbol{\sigma}_{\mathrm{ou}} - \mathbf{C}_{345}^{-1} \mathbf{D}^{\mathrm{T}} \mathbf{e}_{\mathrm{in}}. \end{aligned} \tag{10}$$

Therefore, applying the variational statement (8) according to Eqs. (2), (5)–(7), (10) with the "G"-membership of $\mathbf{e}_{\mathrm{in}}$, carrying out the relevant integrations by parts, not reported here for brevity's sake, with a view to considering the z-integrations through the whole thickness of the laminate and finally taking into account the algebraic/differential manipulations suggested in Messina (2002a), governing differential equations (11), relevant boundary conditions (12) and consistent generalized constitutive equations (13) are obtained as follows:

$$\begin{aligned} \delta u_i &: \frac{1}{A_1} \frac{\partial N_{1i}}{\partial \alpha_1} + \frac{1}{A_2} \frac{\partial N_{121i}}{\partial \alpha_2} - Q_{1i} = \rho^{1j,1i} \ddot{\boldsymbol{u}}_j, \\ \delta v_i &: \frac{1}{A_1} \frac{\partial N_{122i}}{\partial \alpha_1} + \frac{1}{A_2} \frac{\partial N_{2i}}{\partial \alpha_2} - Q_{2i} = \rho^{2j,2i} \ddot{\mathbf{v}}_j, \\ \delta w_i &: \frac{1}{A_1} \frac{\partial V_{1i}}{\partial \alpha_1} + \frac{1}{A_2} \frac{\partial V_{2i}}{\partial \alpha_2} - Q_{3i} = \rho^{3j,3i} \ddot{\mathbf{w}}_j. \end{aligned} \tag{11}$$

$$\begin{aligned} &\text{Along } \alpha_1 = \alpha_1^{\mathrm{start}}, \alpha_1^{\mathrm{end}} \text{ for any } \alpha_2 : N_{1i} = 0 \text{ or } u_i,\ N_{122i} = 0 \text{ or } v_i,\ V_{1i} = 0 \text{ or } w_i. \\ &\text{Along } \alpha_2 = \alpha_2^{\mathrm{start}}, \alpha_2^{\mathrm{end}} \text{ for any } \alpha_1 : N_{121i} = 0 \text{ or } u_i,\ N_{2i} = 0 \text{ or } v_i,\ V_{2i} = 0 \text{ or } w_i. \end{aligned} \tag{12}$$

$$\begin{pmatrix} \mathbf{N}_1 \\ \mathbf{N}_2 \\ \mathbf{N}_{121} \\ \mathbf{N}_{122} \\ \mathbf{V}_1 \\ \mathbf{V}_2 \\ \mathbf{Q}_1 \\ \mathbf{Q}_2 \\ \mathbf{Q}_3 \end{pmatrix} = \begin{bmatrix} \overline{\mathbf{C}}_{11} & \overline{\mathbf{C}}_{12} & \overline{\mathbf{C}}_{13} & \overline{\mathbf{C}}_{14} & \mathbf{0} & \mathbf{0} & \mathbf{0} & \mathbf{0} & \overline{\mathbf{C}}_{19} \\ & \overline{\mathbf{C}}_{22} & \overline{\mathbf{C}}_{23} & \overline{\mathbf{C}}_{24} & \mathbf{0} & \mathbf{0} & \mathbf{0} & \mathbf{0} & \overline{\mathbf{C}}_{29} \\ & & \overline{\mathbf{C}}_{33} & \overline{\mathbf{C}}_{34} & \mathbf{0} & \mathbf{0} & \mathbf{0} & \mathbf{0} & \overline{\mathbf{C}}_{39} \\ & & & \overline{\mathbf{C}}_{44} & \mathbf{0} & \mathbf{0} & \mathbf{0} & \mathbf{0} & \overline{\mathbf{C}}_{49} \\ & & & & \overline{\mathbf{C}}_{55} & \overline{\mathbf{C}}_{56} & \overline{\mathbf{C}}_{57} & \overline{\mathbf{C}}_{58} & \mathbf{0} \\ & \text{sym} & & & & \overline{\mathbf{C}}_{66} & \overline{\mathbf{C}}_{67} & \overline{\mathbf{C}}_{68} & \mathbf{0} \\ & & & & & & \overline{\mathbf{C}}_{77} & \overline{\mathbf{C}}_{78} & \mathbf{0} \\ & & & & & & & \overline{\mathbf{C}}_{88} & \mathbf{0} \\ & & & & & & & & \overline{\mathbf{C}}_{99} \end{bmatrix} \cdot \begin{pmatrix} \mathbf{u}_{,\alpha 1}/A_1 \\ \mathbf{v}_{,\alpha 2}/A_2 \\ \mathbf{u}_{,\alpha 2}/A_2 \\ \mathbf{v}_{,\alpha 1}/A_1 \\ \mathbf{w}_{,\alpha 1}/A_1 \\ \mathbf{w}_{,\alpha 2}/A_2 \\ \mathbf{u} \\ \mathbf{v} \\ \mathbf{w} \end{pmatrix}. \tag{13}$$

It is interesting to notice the effort that was made in order to present a set of equations (11)–(13) in the same form as reported in Messina (2002a). In particular, the relevant equations described in Messina (2002a), for multilayered plates, can be obtained through Eqs. (11)–(13) by substituting the coordinates and magnitudes of the shell $(\alpha_1, \alpha_2, A_1, A_2)$ with $(x, y, 1, 1)$. However, such a correspondence involves the quantities quoted in (11)–(13) which are more generalized with respect to Messina (2002a). This further generalization is put forth in the following equations:

$$\begin{aligned}
(N_{1i}, N_{2i}) &= \int_{-h/2}^{h/2} (\sigma_1, \sigma_2)(\Phi_{1i}, \Phi_{2i})(h_2, h_1)\,\mathrm{d}z, \\
(N_{121i}, N_{122i}) &= \int_{-h/2}^{h/2} \tau_{12}(\Phi_{1i}, \Phi_{2i})(h_1, h_2)\,\mathrm{d}z, \\
(V_{1i}, V_{2i}) &= \int_{-h/2}^{h/2} \Phi_{3i}(\tau_{1zp}, \tau_{2zp})(\Psi_{2p}, \Psi_{1p})(h_2, h_1)\,\mathrm{d}z, \\
(Q_{1i}, Q_{2i}) &= \int_{-h/2}^{h/2} (\Phi'_{1i} h_1 h_2 - h_2 \Phi_{1i}/R_1, \Phi'_{2i} h_1 h_2 - h_1 \Phi_{2i}/R_2)(\Psi_{2p}, \Psi_{1p})(\tau_{1zp}, \tau_{2zp})\,\mathrm{d}z, \\
Q_{3i} &= \int_{-h/2}^{h/2} \Phi'_{3i} h_1 h_2 \Psi_{3p} \sigma_{zp} + \Phi_{3i}(\sigma_1 h_2/R_1 + \sigma_2 h_1/R_2)\,\mathrm{d}z.
\end{aligned} \tag{14}$$

$$\rho^{lm,nq} = \int_{-h/2}^{h/2} \rho h_1 h_2 \Phi_{lm} \Phi_{nq}\,\mathrm{d}z \tag{15}$$

as well as in the matrices quoted in (13) ($\overline{\mathbf{C}}_{ij}$), which are reported in Appendix A and $(\ )'$ that indicates $\mathrm{d}(\ )/\mathrm{d}z$. In this respect, the vector on the right-hand-side in (13) is an assembled vector with ordered corresponding displacement components (6), whilst the vector on the left-hand-side is an assembled vector of ordered corresponding resultant stresses (14). Thus, based on the definitions regarding the resultant stresses (14), (15) and on the stiffness terms ($\overline{\mathbf{C}}_{ij}$ in Appendix A), the relevant equations presented by Messina (2002a) can be obtained by setting $(1/R_1, 1/R_2) = (0, 0)$.

3. The global piecewise-smooth functions (GPSfs)

The theory developed in Section 2 has been introduced without mentioning the nature of the global approximating functions, i.e.:

$$\begin{cases} \Phi(z)_{1i}, \Phi(z)_{2i}, \Phi(z)_{3i}; & \text{(a) : for the displacement components,} \\ \Psi(z)_{1i}, \Psi(z)_{2i}, \Psi(z)_{3i}; & \text{(b) : for the transverse stress components,} \end{cases} \tag{16}$$

to which, the responsibility of fulfilling the external boundary conditions (on the top and bottom of the multilayered shell) and internal ones (continuity requirements at the interlaminar interfaces of the layers that are considered as perfectly bonded together) is entrusted. This particular task is not immediately applicable whenever classical approximating functions are used in (16) (that is, Fourier series, Legendre series or other classes of independent functions (see for example Sansone, 1959; Chihara, 1978). Indeed, the unknown distributions across the thickness, the problem which is being dealt with, are piecewise smooth. Therefore, if such an aspect is not taken into account by the approximating functions the convergence could be compromised by a behavior that is typical of Gibbs phenomenon (the series can oscillate in the neighborhood of the discontinuities) thus, reducing the performances of the model.

Fig. 2a illustrates a set of three global approximating functions $(f(\zeta)_1, f(\zeta)_2, f(\zeta)_3)$ defined in the global domain $[\zeta_0 = -1/2, \zeta_3 = +1/2]$. They were extracted by a complete base made of orthogonal polynomials

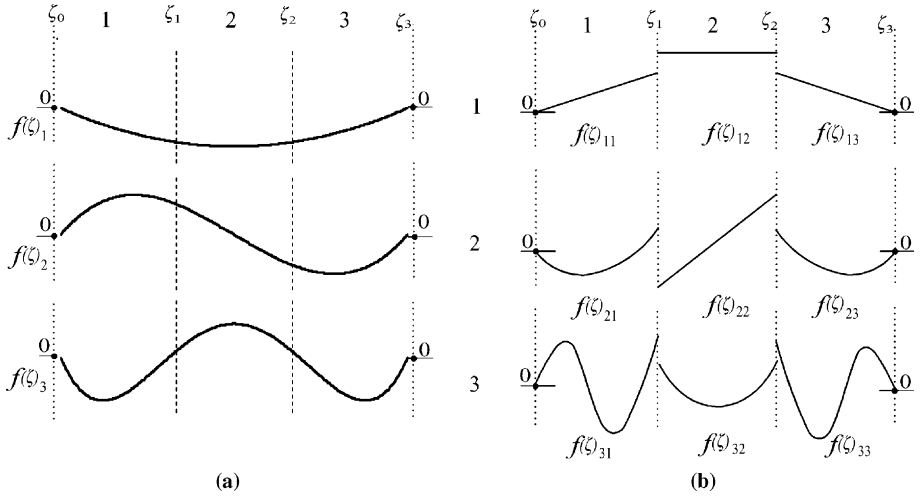

Fig. 2. Global and local approximating functional components for a C^0-continuous function.

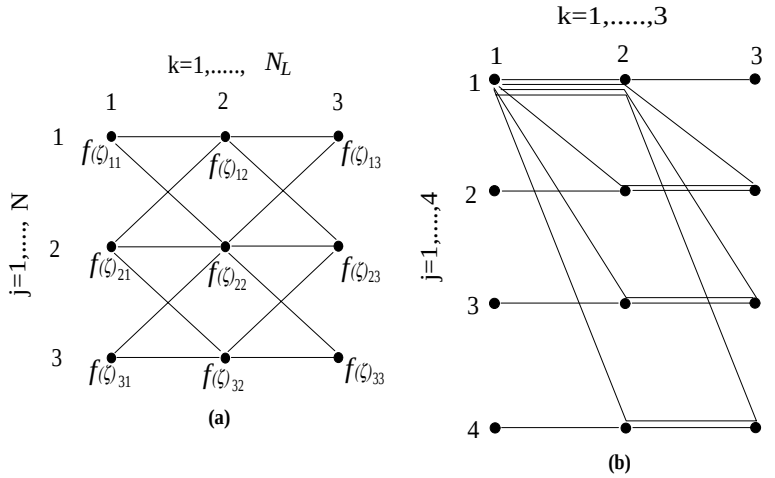

Fig. 3. Representation of extractable dependent or independent paths of GPSFs.

and defined SS to recall the essential type boundary conditions in freely vibrating plates as originally used by Bath (1985) and Dickinson and Di Blasio (1986). If such functions are linearly superimposed in a wise mathematical sense they could approximate a function $f(\zeta)$ that fulfills the following boundary conditions:

$$f(\zeta_0) = f(\zeta_3) = 0. \tag{17}$$

If the function $f(\zeta)$ is piecewise smooth in the three different sub-domains $[(\zeta_0, \zeta_1), (\zeta_1, \zeta_2), (\zeta_2, \zeta_3)]$, the approximation to $f(\zeta)$, through the functions of Fig. 2a, is not efficient with respect to the number of

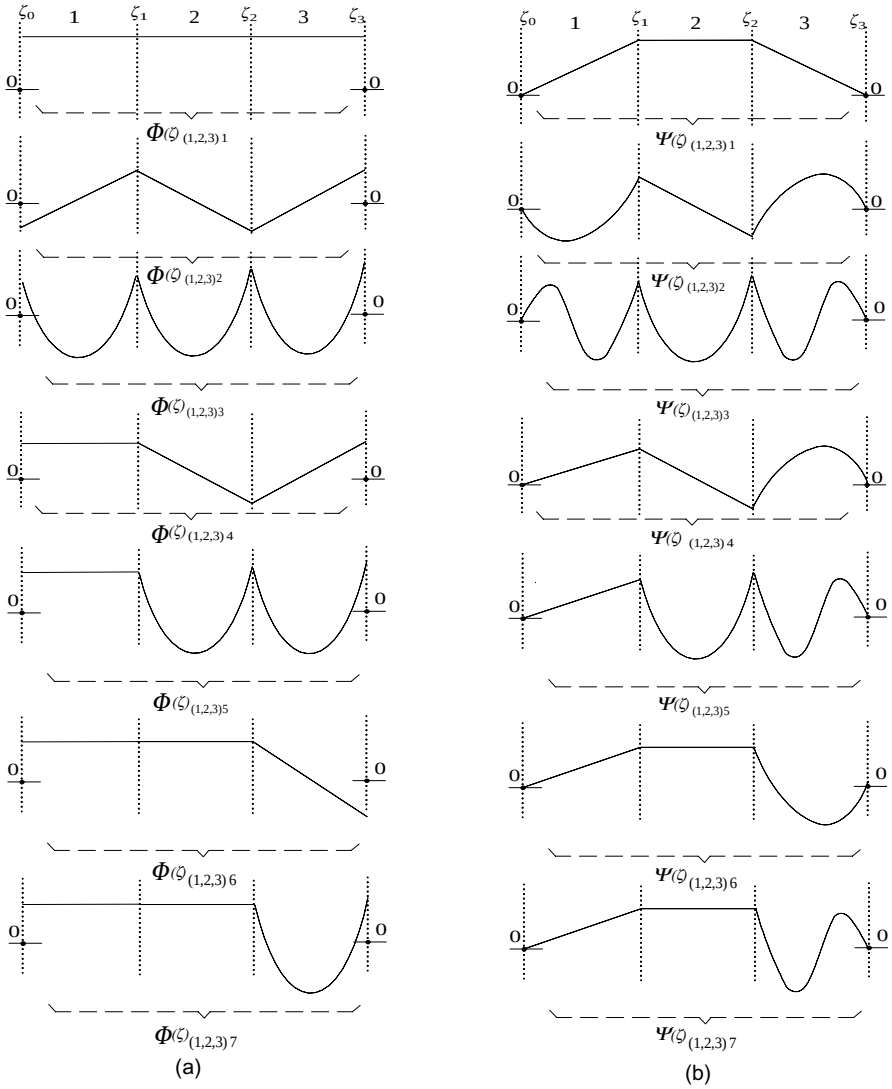

Fig. 4. Selection of $N_L(N-1)+1$ linearly independent GPSFs at an expansion-level $N = 3$ in $N_L = 3$ sub-domains for displacement and stress components.

functions needed. In this regard, the problem could be re-handled through local functional components (Fig. 2b). However, this would need the introduction of continuity requirements in (ζ_1, ζ_2) thus also avoiding a global formulation. In this respect, Messina (2002a) raised the question whether the possibility of extracting a base from Fig. 2b to take into account a global approximation of piecewise smooth functions exists. The question is admissible because any single local polynomial can be scaled to join the contiguous ones. The process originates a chain of local functions that constitute a global approximating function (GPSF). The GPSF would thus be piecewise smooth and an unknown piecewise smooth function could be globally approximated. With regard to such chains, that are represented as graphs in Fig. 3, Messina (2002a) also pointed out that there exists an enormous number of chains (Fig. 3a), but, only $N_L(N-1)+1$ are linearly independent (Fig. 3b); being $N(=N_u=N_\sigma)$ the maximum number used in the functional expansion and N_L the number of sub domains. The patterns indicated in Fig. 3b were used as global approximating functions in the mixed plate model by Messina (2002a) and an excellent performance was obtained. Therefore, according to the encouraging results obtained in the mixed plate model developed in Messina (2002a), the GPSFs are still used in conjunction with the analytical shell model developed in Section 2 of this work.

Namely, the graph of Fig. 3b has been used to extract, among FF local functional components, $N_L(N-1)+1$ global approximating functions under the guise of components (16a). In this way the GPSFs, which are obtained by joining FF local functions, are not constrained to fulfill any condition at the boundaries (top and bottom of the shell). The functional components concerning the transverse stresses (16b) are also obtained by using the graph of Fig. 3b. However, in this latter case, the local functional components must be zero at the boundaries in order to nullify the transverse stresses ($\boldsymbol{\sigma}_{ou}=\mathbf{0}$) on the bottom and top of the shell. Therefore, the extreme local functional components should be SF and FS functions. Fig. 4 clarifies the nature of the GPSFs (16) herein used when the expansion level is $N=3$ in an arrangement of three sub domains (i.e. layers).

4. Freely vibrating cross-ply shells: numerical results

In this section, the analytical model obtained in Section 2 is tested in conjunction with the GPSFs introduced in Messina (2002a), which are briefly reassumed in Section 3. It is stressed that the GPSFs should not be considered as the only possible choice. Indeed, in Section 2 a theory dealing with freely vibrating shells, virtually made of a single layer and having its constant piecewise elastic constant through the thickness, was developed without restricting the class of global functions that could be used. The leading characteristic of the theory is that the mathematical difficulty of fulfilling the physical requirements of the problem (external and internal boundary conditions) belongs to the global approximating functions (16) and these can be whatever, providing that they are consistent with the mentioned physical requirements.

In order to test the good behavior of the analytical model (11)–(15), freely vibrating cross-ply shells, which are subjected to a certain class of simply supported constraints, are herein taken into account. These conditions allow the extraction of exact solutions that can be compared with existing ones as evaluated by others investigators. As far as the three-dimensional simply supported boundary conditions are concerned, Eq. (18) reports the relevant mathematical expression.

$$\alpha_1=0,\quad L_1: V=W=0,\quad \sigma_1=0;\quad \alpha_2=0,\quad L_2: U=W=0,\quad \sigma_2=0 \tag{18}$$

with a convenient metric based on a system of curvilinear coordinates having L_1 and L_2 as lateral lengths of the shell and $\alpha_{1,2}$ starting from a corner where $\alpha_{1,2}=0$.

Three-dimensional boundary conditions (18) correspond to the following two-dimensional ones in an approximate sense:

$$\alpha_1 = 0, \quad L_1 : v_i = w_i = 0, \quad N_{1i} = 0; \quad \alpha_2 = 0, \quad L_2 : u_i = w_i = 0, \quad N_{2i} = 0. \tag{19}$$

These latter (19) are exactly fulfilled for cross-ply shells when the following displacement field is taken into consideration:

$$\begin{cases} u(\alpha_1, \alpha_2; t)_i = A^{ui} \cdot \cos\left(\dfrac{m\pi\alpha_1}{L_1}\right) \cdot \sin\left(\dfrac{n\pi\alpha_2}{L_2}\right) \cdot \cos(\omega_{mn} t), \\ v(\alpha_1, \alpha_2; t)_i = A^{vi} \cdot \sin\left(\dfrac{m\pi\alpha_1}{L_1}\right) \cdot \cos\left(\dfrac{n\pi\alpha_2}{L_2}\right) \cdot \cos(\omega_{mn} t), \\ w(\alpha_1, \alpha_2; t)_i = A^{wi} \cdot \sin\left(\dfrac{m\pi\alpha_1}{L_1}\right) \cdot \sin\left(\dfrac{n\pi\alpha_2}{L_2}\right) \cdot \cos(\omega_{mn} t). \end{cases} \tag{20}$$

Based on the assumed displacement components of equations (20) put together with Eqs. (11), (13), similarly to Messina (2002a) the following generalized eigenvalue problem (21) can be set to extract the exact circular frequencies (ω_{mn}):

$$\det\left(\mathbf{K} - \omega_{mn}^2 \mathbf{M}\right) = 0. \tag{21}$$

Eq. (21) was solved once global approximating functions were chosen. In case of GPSFs both Φ- and Ψ-functions corresponded to that illustrated in Fig. 4. However, before illustrating the numerical tests it is stressed that whenever discontinuities are not present in a multilayered plate or shell (for example homogeneous isotropic or single layer laminates), simple orthogonal polynomials, such as FF and SS bases (e.g. Messina and Soldatos, 1999a,b) should be used in place of GPSFs as Φ- and Ψ-functions, respectively. Here, for brevity's sake, only the more complicated cases dealing with multilayered plates and shells will be illustrated. This void should not be retained a limiting factor of the present analysis because single-layer laminates are particular cases of multilayered ones as Messina (2002b) already illustrated through the analysis of freely vibrating plates.

With respect to all numerical tests considered, Table 1 constitutes an outline. In particular, it recaps the relevant non-dimensional frequency parameters (ω^*) and the material properties used in all the numerical evaluations. As far as the material constants for Tables 2–5 are concerned, they were identical to the

Table 1
Frequency parameters and material properties

Reference tables	ω^*	Elastic constants	Element analyzed
Tables 2–4	$\omega R_1\sqrt{\rho/E_2}$	$E_1 = 25E_2$, $E_2 = E_3$, $G_{12} = G_{13} = 0.5E_2$, $G_{23} = 0.2E_2$, $\nu_{12} = \nu_{13} = \nu_{23} = 0.25$	Multilayered laminates: cylindrical, spherical and saddle-shape
Table 5	$\omega L_1\sqrt{\rho/E_2}$	$E_1 = 25E_2$, $E_2 = E_3$, $G_{12} = G_{13} = 0.5E_2$, $G_{23} = 0.2E_2$, $\nu_{12} = 0.25$, $\nu_{31} = 0.03$, $\nu_{23} = 0.4$	Two-layers circular cylindrical shells
Tables 6–10	$\omega\frac{L_1^2}{h}\sqrt{\frac{\rho}{12E_1(1-\nu_{12}\nu_{21})}}$	Graphite/epoxy AS4/3501-6: $E_1 = 14.9E_2$, $E_2 = E_3$, $G_{12} = G_{13} = 0.543E_2$, $G_{23} = 0.328E_2$, $\nu_{12} = \nu_{13} = 0.31$, $\nu_{23} = 0.52$ E-glass/epoxy: $E_1 = 2.45E_2$, $E_2 = E_3$, $G_{12} = G_{13} = 0.48E_2$, $G_{23} = 0.342E_2$, $\nu_{12} = \nu_{13} = 0.23$, $\nu_{23} = 0.462$	Two and three-layers plates and shells (cylindrical, spherical and saddle-shape)

Table 2
Frequency parameters, ω^*, of cross-ply circular cylindrical laminates for different number of layers ($h/L_1 = 0.1$, $L_1/R_1 = L_2/R_1 = 0.5$)

(m,n): Mode	2	3	4	5	10
M3D					
(1,1): I	1.8971 (4)	2.3112 (4)	2.3415 (4)	2.4231 (4)	2.4930 (3)
(1,1): II	18.813 (3)	18.394 (3)	21.545 (3)	20.531 (3)	22.387 (3)
(1,1): III	20.169 (4)	26.051 (3)	22.902 (3)	25.181 (3)	23.694 (3)
(1,2): I	4.4492 (4)	3.7989 (4)	4.9620 (4)	4.4822 (4)	5.3017 (3)
(1,3): I	7.8195 (4)	6.3115 (5)	8.0752 (4)	7.2057 (4)	8.5254 (4)
(2,1): I	4.3485 (4)	5.5914 (4)	4.8493 (4)	5.5428 (4)	5.1853 (3)
(2,2): I	6.0384 (4)	6.3622 (5)	6.5486 (4)	6.6923 (4)	6.9739 (4)
Huang (1995)					
(1,1): I	1.8971	2.3112	2.3415	2.4231	2.4930
(1,1): II	18.813	18.574	21.545	20.736	22.387
(1,1): III	20.169	25.781	22.902	24.925	23.694
(1,2): I	4.4492	3.7984	4.9620	4.4822	5.3017
(1,3): I	7.8195	6.3115	8.0752	7.2057	8.5254
(2,1): I	4.3485	5.5914	4.8493	5.5428	5.1853
(2,2): I	6.0384	6.3622	6.5486	6.6923	6.9739

Table 3
First frequency parameters, ω^*, of cross-ply spherical laminates for different number of layers ($h/L_1 = 0.1$, $L_1/R_1 = L_2/R_1 = 0.2$)

(m,n)	2	3	4	5	10
M3D					
(1,1)	4.6240 (4)	5.8425 (4)	5.8072 (4)	6.1092 (4)	6.2295 (3)
(1,2)	10.753 (4)	9.2157 (4)	12.134 (4)	10.982 (4)	13.050 (3)
(1,3)	19.130 (6)	15.383 (4)	19.846 (4)	17.689 (4)	21.042 (4)
(2,1)	10.864 (4)	14.138 (4)	12.189 (4)	14.013 (4)	13.076 (3)
(2,2)	14.909 (4)	15.972 (4)	16.298 (4)	16.791 (4)	17.432 (3)
Huang (1995)					
(1,1)	4.6238	5.8423	5.8070	6.1090	6.2293
(1,2)	10.753	9.2156	12.134	10.982	13.050
(1,3)	19.130	15.383	19.846	17.689	21.042
(2,1)	10.864	14.138	12.188	14.013	13.076
(2,2)	14.909	15.972	16.298	16.791	17.432

Table 4
First frequency parameters, ω^*, of cross-ply saddle-shape laminates for different number of layers ($R_2 = -R_1$, $h/L_1 = 0.1$, $L_1/R_1 = L_2/R_1 = 0.5$)

(m,n)	2	3	4	5	10
M3D					
(1,1)	1.7555 (4)	2.1737 (4)	2.2021 (4)	2.2797 (3)	2.3458 (3)
(1,2)	4.4072 (4)	3.6693 (4)	4.8822 (4)	4.3591 (4)	5.2003 (3)
(1,3)	7.8542 (4)	6.2275 (4)	8.0499 (4)	4.1235 (4)	8.4689 (3)
(2,1)	4.4072 (4)	5.5997 (4)	4.8822 (4)	5.5492 (4)	5.2003 (3)
(2,2)	6.0480 (4)	6.2956 (4)	6.5143 (4)	6.6216 (4)	6.9148 (4)
Huang (1995)					
(1,1)	1.7576	2.1761	2.2040	2.2819	2.3477
(1,2)	4.4079	3.6706	4.8830	4.3602	5.2011
(1,3)	7.8545	6.2281	8.0503	7.1240	8.4692
(2,1)	4.4077	5.6001	4.8826	5.5495	5.2006
(2,2)	6.0483	6.2959	6.5145	6.6218	6.9151

Table 5
First frequency parameters, ω^*, of cross-ply [0°/90°], circular cylindrical shells for different R_2/L_1 and h/L_1 ratios ($m = n = 1$, $L_2 = L_1$)

h/L_1	R_2/L_1	Ye and Soldatos (1994)	Wu et al. (1996)[a]	M3D, N		
				2	4	6
0.05	1	0.79316	0.79307	0.79343404	0.79322115	0.79322115
	5	0.49346	0.49331	0.49335600	0.49335352	0.49335352
	10	0.47959	0.47948	0.47950803	0.47951734	0.47951734
0.1	1	1.06973	1.06875	1.07020	1.06973	1.06973
	5	0.90616	0.90573	0.90605	0.90617	0.90617
	10	0.89778	0.89740	0.89763	0.89778	0.89778
0.15	1	1.34537	1.34070	1.34565	1.34534	1.34534
	5	1.24524	1.24210	1.24463	1.24523	1.24523
	10	1.23707	1.23413	1.23644	1.23707	1.23707

[a] ε^6-order solution.

Table 6
First frequency parameters, ω^*, of cross-ply square laminated plates for different h/L_1 ratios

	h/L_1	(m,n)				
		(1,1)	(1,2)	(1,3)	(2,1)	(2,2)
Graphite/epoxy						
[0°/90°]	1/100	7.7481 (4)	20.933 (2)	44.083 (4)	20.933 (2)	30.934 (4)
	1/50	7.7335 (4)	20.817 (4)	43.560 (4)	20.817 (4)	30.704 (4)
	1/10	7.3126 (4)	17.990 (4)	33.307 (4)	17.990 (4)	25.509 (4)
	1/5	6.3773 (4)	13.679 (4)	22.523 (4)	13.679 (4)	18.597 (4)
[0°/90°/0°]	1/100	11.031 (2)	18.001 (3)	32.472 (4)	39.557 (2)	43.895 (3)
	1/50	10.974 (3)	17.910 (4)	32.236 (4)	38.744 (3)	43.017 (4)
	1/10	9.5483 (4)	15.681 (4)	26.862 (4)	25.873 (4)	29.378 (4)
	1/5	7.3445 (4)	12.226 (4)	19.667 (4)	16.164 (4)	19.098 (4)
E-glass/epoxy						
[0°/90°]	1/100	14.457 (2)	37.001 (3)	75.266 (4)	37.001 (3)	57.758 (2)
	1/50	14.440 (2)	36.885 (4)	74.789 (4)	36.885 (4)	57.480 (4)
	1/10	13.916 (4)	33.765 (4)	63.611 (4)	33.765 (4)	50.541 (4)
	1/5	12.635 (4)	27.865 (4)	47.659 (4)	27.865 (4)	39.429 (4)
[0°/90°/0°]	1/100	15.164 (2)	33.697 (2)	65.658 (3)	43.960 (3)	60.572 (3)
	1/50	15.143 (2)	33.607 (3)	65.329 (3)	43.769 (3)	60.246 (3)
	1/10	14.532 (4)	31.133 (4)	57.209 (4)	38.839 (4)	52.267 (4)
	1/5	13.067 (4)	26.200 (4)	44.395 (4)	30.512 (4)	40.022 (4)
Leissa and Narita (1989)		15.193	33.773	65.835	44.054	60.770

constants referring to those few existing results used for the comparisons. Whilst, for Tables 6–10, dealing with new results, the elastic constants were chosen among certain fiber reinforced materials used in several engineering applications. This latter choice was addressed towards two materials that are characterized by an extremely anisotropic (axial to transverse) module (graphite/epoxy: AS4/3501-6) and a lesser

Table 7
First frequency parameters, ω^*, of cross-ply circular cylindrical laminates ($L_1/R_1 = L_2/R_1 = 0.2$) for different h/L_1 ratios

	h/L_1	(m,n)				
		(1,1)	(1,2)	(1,3)	(2,1)	(2,2)
Graphite/epoxy						
[0°/90°]	1/100	14.595 (2)	30.991 (4)	53.250 (4)	21.814 (2)	33.319 (4)
	1/50	9.8936 (2)	23.643 (4)	45.838 (4)	21.080 (3)	31.341 (4)
	1/10	7.4412 (4)	18.129 (4)	33.411 (5)	18.116 (4)	25.671 (4)
	1/5	6.4599 (4)	13.761 (5)	22.593 (5)	13.800 (4)	18.736 (4)
[0°/90°/0°]	1/100	16.487 (2)	29.763 (2)	45.888 (4)	39.889 (2)	45.532 (3)
	1/50	12.527 (2)	21.435 (4)	36.036 (4)	38.785 (3)	43.396 (3)
	1/10	9.5743 (4)	15.807 (4)	27.004 (4)	25.839 (4)	29.365 (4)
	1/5	7.3314 (4)	12.246 (4)	19.699 (4)	16.144 (4)	19.086 (4)
E-glass/epoxy						
[0°/90°]	1/100	28.770 (2)	54.975 (3)	88.091 (4)	38.709 (3)	62.876 (3)
	1/50	19.035 (2)	41.826 (3)	77.726 (4)	37.381 (4)	58.803 (4)
	1/10	14.133 (4)	33.923 (4)	63.645 (4)	33.876 (4)	50.713 (4)
	1/5	12.728 (4)	27.939 (4)	47.695 (4)	27.994 (4)	39.594 (4)
[0°/90°/0°]	1/100	29.039 (2)	54.679 (3)	83.262 (3)	45.029 (3)	65.402 (3)
	1/50	19.521 (3)	39.874 (3)	70.130 (4)	43.990 (2)	61.444 (3)
	1/10	14.677 (3)	31.375 (4)	57.396 (4)	38.794 (4)	52.268 (4)
	1/5	13.068 (4)	26.244 (4)	44.438 (4)	30.473 (4)	40.000 (4)

Table 8
First frequency parameters, ω^*, of cross-ply spherical laminates ($L_1/R_1 = L_2/R_1 = 0.2$) for different h/L_1 ratios

	h/L_1	(m,n)				
		(1,1)	(1,2)	(1,3)	(2,1)	(2,2)
Graphite/epoxy						
[0°/90°]	1/100	25.882 (2)	35.453 (2)	55.201 (4)	36.051 (3)	39.576 (2)
	1/50	14.540 (3)	25.090 (4)	46.305 (4)	25.534 (4)	33.041 (4)
	1/10	7.6554 (4)	18.048 (4)	33.228 (5)	18.264 (4)	25.575 (4)
	1/5	6.4429 (4)	13.637 (4)	22.448 (5)	13.779 (4)	18.603 (4)
[0°/90°/0°]	1/100	26.915 (2)	34.673 (2)	48.500 (3)	48.324 (2)	50.267 (3)
	1/50	16.424 (2)	23.199 (4)	36.872 (4)	41.083 (3)	44.668 (4)
	1/10	9.7894 (4)	15.894 (4)	27.039 (4)	25.953 (4)	29.426 (4)
	1/5	7.3922 (4)	12.268 (4)	19.707 (4)	16.180 (4)	19.104 (4)
E-glass/epoxy						
[0°/90°]	1/100	51.798 (2)	63.052 (3)	90.971 (4)	64.861 (3)	76.214 (3)
	1/50	28.722 (2)	44.470 (4)	78.421 (4)	45.761 (4)	62.561 (4)
	1/10	14.694 (4)	33.889 (4)	63.459 (4)	34.280 (4)	50.709 (4)
	1/5	12.802 (4)	27.799 (4)	47.493 (4)	28.051 (4)	39.454 (4)
[0°/90°/0°]	1/100	51.843 (2)	63.500 (3)	86.851 (4)	66.695 (3)	78.262 (3)
	1/50	29.011 (2)	43.001 (3)	71.185 (4)	50.382 (3)	65.078 (3)
	1/10	15.272 (3)	31.517 (4)	57.422 (4)	39.081 (4)	52.427 (4)
	1/5	13.225 (4)	26.277 (4)	44.439 (4)	30.555 (4)	40.046 (4)

fiber-dominated material (E-glass/epoxy). Both the materials, that are considered as transversely isotropic, were adopted as reasonable mean values among the suggested ones by the specialized literature

Table 9
First frequency parameters, ω^*, of cross-ply saddle-shape laminates ($R_2 = -R_1$, $L_1/R_1 = L_2/R_1 = 0.2$) for different h/L_1 ratios

	h/L_1	(m,n)				
		(1,1)	(1,2)	(1,3)	(2,1)	(2,2)
Graphite/epoxy						
[0°/90°]	1/100	7.6913 (4)	26.971 (4)	51.394 (4)	26.971 (4)	30.917 (2)
	1/50	7.6898 (4)	22.411 (4)	45.371 (4)	22.411 (4)	30.738 (4)
	1/10	7.3607 (4)	18.180 (4)	33.558 (4)	18.180 (4)	25.773 (4)
	1/5	6.4823 (4)	13.858 (4)	22.716 (5)	13.858 (4)	18.854 (4)
[0°/90°/0°]	1/100	10.937 (2)	25.251 (3)	43.381 (3)	42. 847 (2)	43.801 (3)
	1/50	10.880 (2)	19.918 (3)	35.234 (4)	39.528 (3)	42.925 (4)
	1/10	9.4666 (4)	15.706 (4)	26.944 (4)	25.846 (4)	29.316 (4)
	1/5	7.2823 (4)	12.206 (4)	19.674 (4)	16.133 (4)	19.060 (4)
E-glass/epoxy						
[0°/90°]	1/100	14.331 (2)	47.702 (3)	85.356 (3)	47.702 (3)	57.664 (3)
	1/50	14.324 (3)	39.580 (4)	77.018 (4)	39.580 (4)	57.429 (4)
	1/10	13.884 (4)	33.893 (4)	63.756 (4)	33.893 (4)	50.742 (4)
	1/5	12.676 (4)	28.016 (4)	47.848 (4)	28.016 (4)	39.701 (4)
[0°/90°/0°]	1/100	15.022 (3)	46.591 (3)	79.830 (3)	53.196 (3)	60.430 (3)
	1/50	15.001 (2)	37.175 (3)	69.090 (4)	46.177 (3)	60.104 (4)
	1/10	14.396 (3)	31.188 (4)	57.307 (4)	38.850 (4)	52.145 (4)
	1/5	12.945 (4)	26.159 (4)	44.395 (4)	30.462 (4)	39.930 (4)

Table 10
First frequency parameters, ω^*, of cross-ply laminates for different h/L_1 and L_1/R_1 ratios ($m = n = 1$; graphite/epoxy)

	h/L_1	$(L_1/R_1 = L_2/R_1)$			
		0.02	0.2	0.5	1
$R_2 = \infty$ (*cylindrical*)					
[0°/90°]	1/10	7.3190 (4)	7.4412 (4)	7.8913 (4)	9.1606 (4)
	1/5	6.3853 (4)	6.4599 (4)	6.5956 (4)	6.8474 (4)
[0°/90°/0°]	1/10	9.5486 (4)	9.5743 (4)	9.7087 (4)	10.167 (4)
	1/5	7.3444 (4)	7.3314 (4)	7.2653 (4)	7.0675 (4)
$R_2 = R_1$ (*spherical*)					
[0°/90°]	1/10	7.3161 (4)	7.6554 (4)	9.1996 (4)	12.901 (4)
	1/5	6.3780 (4)	6.4429 (4)	6.7689 (4)	7.7346 (4)
[0°/90°/0°]	1/10	9.5508 (4)	9.7894 (4)	10.930 (4)	13.917 (3)
	1/5	7.3450 (4)	7.3922 (4)	7.6316 (4)	8.3602 (4)
$R_2 = -R_1$ (*saddle-shape*)					
[0°/90°]	1/10	7.3232 (4)	7.3607 (4)	7.1859 (4)	6.2893 (4)
	1/5	6.3926 (4)	6.4823 (4)	6.4275 (4)	5.7726 (4)
[0°/90°/0°]	1/10	9.5475 (4)	9.4666 (4)	9.0509 (4)	7.7243 (4)
	1/5	7.3439 (4)	7.2823 (4)	6.9659 (4)	5.9585 (4)

(e.g. Tsai and Hahn, 1980; Christensen and Zywicz, 1990; Roy and Tsai, 1992; Kelly et al., 1994; Philippidis and Theocaris, 1994; Yuan and Hsieh, 1998; Chao and Chern, 2000; Vinson and Sierakowski, 2002).

The material constants of graphite/epoxy and E-glass/epoxy correspond to the values adopted by Christensen and Zywicz (1990) and Chao and Chern (2000), respectively.

Based on the three-dimensional investigations conducted by Huang (1995), which can be taken into account in this work, Tables 2–4 have been set up as an initial test in the cases of cylindrical, spherical and saddle-shape laminates. Tables 2–4 consider certain laminates that are constructed regularly in the sequence $[0°/90°\ldots]$ with equal layer thickness. The frequency parameters (ω^*) presented in these Tables have to be considered as being obtained by the numerical codes when the convergence for the first five significant figures was achieved. In this respect the corresponding numbers in brackets indicate the number of functional components needed in order to reach the convergence. A perusal of Tables 2–4 highlights that an increasing number of layers gets the convergence with a decreasing order of functional components (N). This aspect seems to be independent from the particular geometry investigated. It can be justified by the reduction of the thickness for each layer which, requires a through-thickness distribution of stress and displacement quantities with an increasing resemblance to piecewise linear trends.

In Tables 2–4 an excellent coincidence can be observed between the results obtained by the present two-dimensional model and the three-dimensional investigation conducted by Huang (1995). In particular, in Tables 2 and 3 the coincidence applies to five significant figures for the majority of the numerical results. Table 4 illustrates a less favorable comparison but still excellent. Moreover, as far as Table 4 is concerned, it is interesting to note that the present two-dimensional model achieves the convergence at the same numerical value when (m,n) is equal to $(1,2)$ or $(2,1)$ for an even number of layers. While this result is physically compatible with the geometry and the layout considered, Huang (1995) evaluated the same relevant values with a slight discrepancy. This would suggest that the results presented through the present model could be slightly more accurate than the results presented by Huang (1995).

A second test that deserves attention corresponds to the numerical evaluation reported in Table 5. In Table 5 a convergence test is illustrated in conjunction with the comparison of the three-dimensional analysis conducted by Ye and Soldatos (1994) and Wu et al. (1996). Table 5 highlights the extreme stability of the present two-dimensional model. Indeed, all the frequency parameters achieved the convergence on the first six significant figures with $N = 4$. Such a convergence is also illustrated up to the first eight figures in a part of the results only to illustrate the efficiency and stability of the method. The comparison with three-dimensional analysis can be considered excellent, particularly with the analysis conducted by Soldatos (1994) for which four or five significant figures are exactly corresponding.

Based on the more than encouraging numerical comparisons illustrated in Tables 2–5, Tables 6–10 have been set up to provide the literature with new results.

In particular, Tables 6–10 illustrate frequency parameters related to laminated plates and shells which have different geometrical shapes and an even and odd number of layers. All the frequency parameters listed in Tables 6–10 are shown with the needed number of functional components (N). Such a number in parenthesis corresponds to the lowest number of functional components (incremented by a unitary step) between two subsequent frequency parameters identically evaluated with the first rounded five significant digits. This choice was retained important in order to compare future alternative models with the performances of the present model also from a computational point of view.

Table 6, that deals with freely vibrating multilayered plates was obtained as a particular case of shell by simply settling $1/R_1 = 1/R_2 = 0$. This table also illustrates that values from the classical plate theory (Leissa and Narita, 1989) are naturally obtained when the thickness of the plate decreases and becomes considerably smaller than a representative length (L_1). This does not apply for thicker plates for which the frequency parameters considerably change.

The numerical evaluations shown in Tables 6–9 illustrate how the convergence ratio can depend on the particular material and geometry considered. Indeed, a slower convergence can be observed for higher frequencies when curved shells (in particular cylindrical and spherical), made up of graphite/epoxy material, are taken into account. However, such a dependence of the convergence rate should not be considered

remarkably significant. Indeed, when the convergence was obtained with $N = 5$ the frequency parameter corresponding to $N = 4$ already had four stable significant digits.

Moreover, it is interesting to notice that Tables 6–9 have a feature in common: as the shells become thicker the frequency parameters, corresponding to an identical stacking pattern, become similar regardless of the different material or shape of the middle plane (for example, for $h/L_1 = 1/5$, an even number of layers, graphite/epoxy laminates and $(m, n) = (2, 2)$: $\omega^* = 18.597$, 18.736, 18.603, 18.804 correspond to plane, cylindrical, spherical and saddle-shape laminates, respectively). The high thickness of the laminate tends to reduce the effect of the curvatures of the shells, which is, however, more dominant for thinner shells. This interpretation is confirmed in Table 10 that, besides providing new results, illustrates the behavior of frequency parameters $(m, n = 1, 1)$ versus increasing $L_{1,2}/R_{1,2}$ ratios. In this table it can be noticed that for $L_{1,2}/R_{1,2} = 0.02$ the relevant frequency parameters are coincident with the first two significant digits, whilst for increasing $L_{1,2}/R_{1,2}$ ratios this coincidence decreases with a more remarkable trend for $h/L_1 = 10$.

5. Closure

In the frame of free vibrations analysis this paper has presented a two-dimensional theory that is able to achieve an arbitrary accuracy for the modelling of laminated doubly curved shells made of monoclinic elastic layers placed in a general, arbitrary, stacking pattern. This constitutes a further generalization of a recent theory (Messina, 2002a) that concerned freely vibrating plates.

The theory has been developed on the base of one of Reissner's variational theorems (Reissner, 1986). Assuming the doubly curved shell is virtually made from a single layer, this paper has developed the model, thus establishing a refined global theory. Such a global characteristic has been made possible by leaving the task of fulfilling internal and external boundary conditions (in the thickness-direction) to certain global approximating functions, which can be chosen independently from the theoretical model.

In this work a recent set of independent functions (GPSFs) (Messina, 2002a) was used as global approximating functions in the numerical simulations for testing the theoretical model (M3D). An extensive number of comparisons was carried out on different geometries, material and layout arrangements. The comparisons clearly showed that the present two-dimensional model can efficiently challenge three-dimensional (exact and approximated ones) analysis, thus also being obviously superior to well known previous global theories (CPT, FSDST and HSDST).

Due to the fact that the GPSFs here used do not have an exclusive right in the developed theoretical model, it would be interesting to leave further investigations open on the suitability of other independent functions that could even improve the convergence rate of the model. Care should be taken for dealing with functional bases that are compatible with external and internal boundary conditions. Finally, since the theoretical model, tested for a class of simply supported boundary conditions and for certain geometries and materials, showed an evident three-dimensional performance it would be interesting to extend the analysis in order to provide the literature with relevant new three-dimensional results. In this respect, the new values added to the literature for several geometrical and material characteristics of shells should be of relevant value.

Acknowledgement

The work reported in this paper was supported by the basic research funds (ex-60%) awarded to the author in 2001 and 2002.

Appendix A

$$
\begin{aligned}
&\overline{\mathbf{C}}_{11} = \int_{-h/2}^{h/2} Q_{11}\frac{h_2}{h_1}\boldsymbol{\Phi}_1\boldsymbol{\Phi}_1^{\mathrm{T}}\,\mathrm{d}z + \mathbf{B}_{32}^{u\mathrm{T}}\mathbf{G}_{33}\mathbf{B}_{32}^{u}, \quad \overline{\mathbf{C}}_{12} = \int_{-h/2}^{h/2} Q_{12}\boldsymbol{\Phi}_1\boldsymbol{\Phi}_2^{\mathrm{T}}\,\mathrm{d}z + \mathbf{B}_{32}^{u\mathrm{T}}\mathbf{G}_{33}\mathbf{B}_{33}^{v},\\
&\overline{\mathbf{C}}_{13} = \int_{-h/2}^{h/2} Q_{16}\boldsymbol{\Phi}_1\boldsymbol{\Phi}_1^{\mathrm{T}}\,\mathrm{d}z + \mathbf{B}_{32}^{u\mathrm{T}}\mathbf{G}_{33}\mathbf{B}_{33}^{u}, \quad \overline{\mathbf{C}}_{14} = \int_{-h/2}^{h/2} Q_{16}\frac{h_2}{h_1}\boldsymbol{\Phi}_1\boldsymbol{\Phi}_2^{\mathrm{T}}\,\mathrm{d}z + \mathbf{B}_{32}^{u\mathrm{T}}\mathbf{G}_{33}\mathbf{B}_{32}^{v},\\
&\overline{\mathbf{C}}_{22} = \int_{-h/2}^{h/2} Q_{22}\frac{h_1}{h_2}\boldsymbol{\Phi}_2\boldsymbol{\Phi}_2^{\mathrm{T}}\,\mathrm{d}z + \mathbf{B}_{33}^{v\mathrm{T}}\mathbf{G}_{33}\mathbf{B}_{33}^{v}, \quad \overline{\mathbf{C}}_{23} = \int_{-h/2}^{h/2} Q_{26}\frac{h_1}{h_2}\boldsymbol{\Phi}_2\boldsymbol{\Phi}_1^{\mathrm{T}}\,\mathrm{d}z + \mathbf{B}_{33}^{v\mathrm{T}}\mathbf{G}_{33}\mathbf{B}_{33}^{u},\\
&\overline{\mathbf{C}}_{24} = \int_{-h/2}^{h/2} Q_{26}\boldsymbol{\Phi}_2\boldsymbol{\Phi}_2^{\mathrm{T}}\,\mathrm{d}z + \mathbf{B}_{33}^{v\mathrm{T}}\mathbf{G}_{33}\mathbf{B}_{32}^{v}, \quad \overline{\mathbf{C}}_{33} = \int_{-h/2}^{h/2} Q_{66}\frac{h_1}{h_2}\boldsymbol{\Phi}_1\boldsymbol{\Phi}_1^{\mathrm{T}}\,\mathrm{d}z + \mathbf{B}_{33}^{u\mathrm{T}}\mathbf{G}_{33}\mathbf{B}_{33}^{u},\\
&\overline{\mathbf{C}}_{34} = \int_{-h/2}^{h/2} Q_{66}\boldsymbol{\Phi}_1\boldsymbol{\Phi}_2^{\mathrm{T}}\,\mathrm{d}z + \mathbf{B}_{33}^{u\mathrm{T}}\mathbf{G}_{33}\mathbf{B}_{32}^{v}, \quad \overline{\mathbf{C}}_{44} = \int_{-h/2}^{h/2} Q_{66}\frac{h_2}{h_1}\boldsymbol{\Phi}_2\boldsymbol{\Phi}_2^{\mathrm{T}}\,\mathrm{d}z + \mathbf{B}_{32}^{v\mathrm{T}}\mathbf{G}_{33}\mathbf{B}_{32}^{v},\\
&\overline{\mathbf{C}}_{19} = \mathbf{B}_{32}^{u\mathrm{T}}\mathbf{G}_{33}\mathbf{B}_{31}^{w} + \frac{1}{R_1}\int_{-h/2}^{h/2} Q_{11}\frac{h_2}{h_1}\boldsymbol{\Phi}_1\boldsymbol{\Phi}_3^{\mathrm{T}}\,\mathrm{d}z + \frac{1}{R_2}\int_{-h/2}^{h/2} Q_{12}\boldsymbol{\Phi}_1\boldsymbol{\Phi}_3^{\mathrm{T}}\,\mathrm{d}z,\\
&\overline{\mathbf{C}}_{29} = \mathbf{B}_{33}^{v\mathrm{T}}\mathbf{G}_{33}\mathbf{B}_{31}^{w} + \frac{1}{R_1}\int_{-h/2}^{h/2} Q_{12}\boldsymbol{\Phi}_2\boldsymbol{\Phi}_3^{\mathrm{T}}\,\mathrm{d}z + \frac{1}{R_2}\int_{-h/2}^{h/2} Q_{22}\frac{h_1}{h_2}\boldsymbol{\Phi}_2\boldsymbol{\Phi}_3^{\mathrm{T}}\,\mathrm{d}z,\\
&\overline{\mathbf{C}}_{39} = \mathbf{B}_{33}^{u\mathrm{T}}\mathbf{G}_{33}\mathbf{B}_{31}^{w} + \frac{1}{R_1}\int_{-h/2}^{h/2} Q_{16}\boldsymbol{\Phi}_1\boldsymbol{\Phi}_3^{\mathrm{T}}\,\mathrm{d}z + \frac{1}{R_2}\int_{-h/2}^{h/2} Q_{26}\frac{h_1}{h_2}\boldsymbol{\Phi}_1\boldsymbol{\Phi}_3^{\mathrm{T}}\,\mathrm{d}z,\\
&\overline{\mathbf{C}}_{49} = \mathbf{B}_{32}^{v\mathrm{T}}\mathbf{G}_{33}\mathbf{B}_{31}^{w} + \frac{1}{R_1}\int_{-h/2}^{h/2} Q_{16}\frac{h_2}{h_1}\boldsymbol{\Phi}_2\boldsymbol{\Phi}_3^{\mathrm{T}}\,\mathrm{d}z + \frac{1}{R_2}\int_{-h/2}^{h/2} Q_{26}\boldsymbol{\Phi}_2\boldsymbol{\Phi}_3^{\mathrm{T}}\,\mathrm{d}z,\\
&\overline{\mathbf{C}}_{55} = \mathbf{B}_{22}^{w\mathrm{T}}\mathbf{G}_{22}\mathbf{B}_{22}^{w}, \quad \overline{\mathbf{C}}_{56} = \mathbf{B}_{22}^{w\mathrm{T}}\mathbf{G}_{12}^{\mathrm{T}}\mathbf{B}_{13}^{w}, \quad \overline{\mathbf{C}}_{57} = \mathbf{B}_{22}^{w\mathrm{T}}\mathbf{G}_{22}\mathbf{B}_{21}^{u}, \quad \overline{\mathbf{C}}_{58} = \mathbf{B}_{22}^{w\mathrm{T}}\mathbf{G}_{12}^{\mathrm{T}}\mathbf{B}_{11}^{v},\\
&\overline{\mathbf{C}}_{66} = \mathbf{B}_{13}^{w\mathrm{T}}\mathbf{G}_{11}\mathbf{B}_{13}^{w}, \quad \overline{\mathbf{C}}_{67} = \mathbf{B}_{13}^{w\mathrm{T}}\mathbf{G}_{12}\mathbf{B}_{21}^{u}, \quad \overline{\mathbf{C}}_{68} = \mathbf{B}_{13}^{w\mathrm{T}}\mathbf{G}_{11}\mathbf{B}_{11}^{v}, \quad \overline{\mathbf{C}}_{77} = \mathbf{B}_{21}^{u\mathrm{T}}\mathbf{G}_{22}\mathbf{B}_{21}^{u};\\
&\overline{\mathbf{C}}_{78} = \mathbf{B}_{21}^{u\mathrm{T}}\mathbf{G}_{12}^{\mathrm{T}}\mathbf{B}_{11}^{v}, \quad \overline{\mathbf{C}}_{88} = \mathbf{B}_{11}^{v\mathrm{T}}\mathbf{G}_{11}\mathbf{B}_{11}^{v},\\
&\overline{\mathbf{C}}_{99} = \mathbf{B}_{31}^{w\mathrm{T}}\mathbf{G}_{33}\mathbf{B}_{31}^{w} + \frac{1}{R_1^2}\int_{-h/2}^{h/2} Q_{11}\frac{h_2}{h_1}\boldsymbol{\Phi}_3\boldsymbol{\Phi}_3^{\mathrm{T}}\,\mathrm{d}z + \cdots + \frac{1}{R_2^2}\int_{-h/2}^{h/2} Q_{22}\frac{h_1}{h_2}\boldsymbol{\Phi}_3\boldsymbol{\Phi}_3^{\mathrm{T}}\,\mathrm{d}z + \frac{2}{R_1R_2}\int_{-h/2}^{h/2} Q_{12}\boldsymbol{\Phi}_3\boldsymbol{\Phi}_3^{\mathrm{T}}\,\mathrm{d}z,
\end{aligned}
\tag{A.1}
$$

where Q_{ij} are the piecewise continuous reduced stiffnesses (Whitney, 1987) and $(\boldsymbol{\Phi}_1, \boldsymbol{\Phi}_2, \boldsymbol{\Phi}_3)$ are vectors assembled with the ordered global approximating functions $(\Phi(z)_{1j}, \Phi(z)_{2j}, \Phi(z)_{3j})$, respectively. The transverse stress components are related to the displacement components through the following equation:

$$
\boldsymbol{\tau} = \mathbf{G}\cdot\mathbf{B}^{u}\cdot\bar{\mathbf{u}} + \mathbf{G}\cdot\mathbf{B}^{v}\cdot\bar{\mathbf{v}} + \mathbf{G}\cdot\mathbf{B}^{w}\cdot\bar{\mathbf{w}}, \tag{A.2}
$$

where the stress and displacement vectors correspond to the following terms:

$$
\begin{aligned}
\boldsymbol{\tau} &= (\tau_{2z1}, \ldots, \tau_{2zN\sigma}; \tau_{1z1}, \ldots, \tau_{1zN\sigma}; \sigma_{z1}, \ldots, \sigma_{zN\sigma})^{\mathrm{T}},\\
\bar{\mathbf{u}} &= (u_1, \ldots, u_{Nu}; u_{1,\alpha1}/A_1, \ldots, u_{Nu,\alpha1}/A_1; u_{1,\alpha2}/A_2, \ldots, u_{Nu,\alpha2}/A_2)^{\mathrm{T}},\\
\bar{\mathbf{v}} &= (v_1, \ldots, v_{Nu}; v_{1,\alpha1}/A_1, \ldots, v_{Nu,\alpha1}/A_1; v_{1,\alpha2}/A_2, \ldots, v_{Nu,\alpha2}/A_2)^{\mathrm{T}},\\
\bar{\mathbf{w}} &= (w_1, \ldots, w_{Nu}; w_{1,\alpha1}/A_1, \ldots, w_{Nu,\alpha1}/A_1; w_{1,\alpha2}/A_2, \ldots, w_{Nu,\alpha2}/A_2)^{\mathrm{T}}
\end{aligned}
\tag{A.3}
$$

and the sub-matrices $(\mathbf{G}, \mathbf{B}^u, \mathbf{B}^v, \mathbf{B}^w)$ that are constituted as follows:

$$\mathbf{G} = \begin{bmatrix} \mathbf{G}_{11} & \mathbf{G}_{12} & 0 \\ \mathbf{G}_{12}^{\mathrm{T}} & \mathbf{G}_{22} & 0 \\ \mathbf{0} & \mathbf{0} & \mathbf{G}_{33} \end{bmatrix} = \begin{bmatrix} \mathbf{A}_{11} & \mathbf{A}_{12} & \mathbf{0} \\ \mathbf{A}_{12}^{\mathrm{T}} & \mathbf{A}_{22} & \mathbf{0} \\ \mathbf{0} & \mathbf{0} & \mathbf{A}_{33} \end{bmatrix}^{-1}, \tag{A.4}$$

$$\begin{cases} \mathbf{A}_{11} = \displaystyle\int_{-h/2}^{h/2} h_1 h_2 E_{11} \cdot \begin{bmatrix} \Psi_{11}\Psi_{11} & \cdots & \Psi_{11}\Psi_{1N\sigma} \\ \vdots & \ddots & \vdots \\ \Psi_{1N\sigma}\Psi_{11} & \cdots & \Psi_{1N\sigma}\Psi_{1N\sigma} \end{bmatrix} \mathrm{d}z, & \mathbf{A}_{12} = \displaystyle\int_{-h/2}^{h/2} h_1 h_2 E_{12} \cdot \begin{bmatrix} \Psi_{21}\Psi_{11} & \cdots & \Psi_{2N\sigma}\Psi_{11} \\ \vdots & \ddots & \vdots \\ \Psi_{21}\Psi_{1N\sigma} & \cdots & \Psi_{2N\sigma}\Psi_{1N\sigma} \end{bmatrix} \mathrm{d}z, \\ \mathbf{A}_{22} = \displaystyle\int_{-h/2}^{h/2} h_1 h_2 E_{22} \cdot \begin{bmatrix} \Psi_{21}\Psi_{21} & \cdots & \Psi_{21}\Psi_{2N\sigma} \\ \vdots & \ddots & \vdots \\ \Psi_{2N\sigma}\Psi_{21} & \cdots & \Psi_{2N\sigma}\Psi_{2N\sigma} \end{bmatrix} \mathrm{d}z, & \mathbf{A}_{33} = \displaystyle\int_{-h/2}^{h/2} h_1 h_2 E_{33} \cdot \begin{bmatrix} \Psi_{31}\Psi_{31} & \cdots & \Psi_{31}\Psi_{3N\sigma} \\ \vdots & \ddots & \vdots \\ \Psi_{3N\sigma}\Psi_{31} & \cdots & \Psi_{3N\sigma}\Psi_{3N\sigma} \end{bmatrix} \mathrm{d}z. \end{cases} \tag{A.5}$$

$$\mathbf{B}^u = \begin{bmatrix} 0 & 0 & 0 \\ \mathbf{B}_{211}^u + \mathbf{B}_{212}^u & 0 & 0 \\ 0 & \mathbf{B}_{32}^u & \mathbf{B}_{33}^u \end{bmatrix}, \quad \mathbf{B}^v = \begin{bmatrix} \mathbf{B}_{111}^v + \mathbf{B}_{112}^v & 0 & 0 \\ 0 & 0 & 0 \\ 0 & \mathbf{B}_{32}^v & \mathbf{B}_{33}^v \end{bmatrix}, \quad \mathbf{B}^w = \begin{bmatrix} 0 & 0 & \mathbf{B}_{13}^w \\ 0 & \mathbf{B}_{22}^w & 0 \\ \mathbf{B}_{311}^w + \mathbf{B}_{312}^w + \mathbf{B}_{313}^w & 0 & 0 \end{bmatrix}, \tag{A.6}$$

$$\begin{cases} \mathbf{B}_{211}^u = \displaystyle\int_{-h/2}^{h/2} h_1 h_2 \begin{bmatrix} \Psi_{21}\Phi'_{11} & \cdots & \Psi_{21}\Phi'_{1Nu} \\ \vdots & \ddots & \vdots \\ \Psi_{2N\sigma}\Phi'_{11} & \cdots & \Psi_{2N\sigma}\Phi'_{1Nu} \end{bmatrix} \mathrm{d}z, & \mathbf{B}_{212}^u = -\frac{1}{R_1} \displaystyle\int_{-h/2}^{h/2} h_2 \begin{bmatrix} \Psi_{21}\Phi_{11} & \cdots & \Psi_{21}\Phi_{1Nu} \\ \vdots & \ddots & \vdots \\ \Psi_{2N\sigma}\Phi_{11} & \cdots & \Psi_{2N\sigma}\Phi_{1Nu} \end{bmatrix} \mathrm{d}z, \\ \mathbf{B}_{32}^u = \displaystyle\int_{-h/2}^{h/2} F_{31} h_2 \cdot \begin{bmatrix} \Psi_{31}\Phi_{11} & \cdots & \Psi_{31}\Phi_{1Nu} \\ \vdots & \ddots & \vdots \\ \Psi_{3N\sigma}\Phi_{11} & \cdots & \Psi_{3N\sigma}\Phi_{1Nu} \end{bmatrix} \mathrm{d}z, & \mathbf{B}_{33}^u = \displaystyle\int_{-h/2}^{h/2} F_{33} h_1 \cdot \begin{bmatrix} \Psi_{31}\Phi_{11} & \cdots & \Psi_{31}\Phi_{1Nu} \\ \vdots & \ddots & \vdots \\ \Psi_{3N\sigma}\Phi_{11} & \cdots & \Psi_{3N\sigma}\Phi_{1Nu} \end{bmatrix} \mathrm{d}z. \end{cases} \tag{A.7}$$

$$\begin{cases} \mathbf{B}_{111}^v = \displaystyle\int_{-h/2}^{h/2} h_1 h_2 \begin{bmatrix} \Psi_{11}\Phi'_{21} & \cdots & \Psi_{11}\Phi'_{2Nu} \\ \vdots & \ddots & \vdots \\ \Psi_{1N\sigma}\Phi'_{21} & \cdots & \Psi_{1N\sigma}\Phi'_{2Nu} \end{bmatrix} \mathrm{d}z, & \mathbf{B}_{112}^v = -\dfrac{1}{R_2} \displaystyle\int_{-h/2}^{h/2} h_1 \begin{bmatrix} \Psi_{11}\Phi_{21} & \cdots & \Psi_{11}\Phi_{2Nu} \\ \vdots & \ddots & \vdots \\ \Psi_{1N\sigma}\Phi_{21} & \cdots & \Psi_{1N\sigma}\Phi_{2Nu} \end{bmatrix} \mathrm{d}z, \\ \mathbf{B}_{32}^v = \displaystyle\int_{-h/2}^{h/2} F_{33} h_2 \cdot \begin{bmatrix} \Psi_{31}\Phi_{21} & \cdots & \Psi_{31}\Phi_{2Nu} \\ \vdots & \ddots & \vdots \\ \Psi_{3N\sigma}\Phi_{21} & \cdots & \Psi_{3N\sigma}\Phi_{2Nu} \end{bmatrix} \mathrm{d}z, & \mathbf{B}_{33}^v = \displaystyle\int_{-h/2}^{h/2} F_{32} h_1 \cdot \begin{bmatrix} \Psi_{31}\Phi_{21} & \cdots & \Psi_{31}\Phi_{2Nu} \\ \vdots & \ddots & \vdots \\ \Psi_{3N\sigma}\Phi_{21} & \cdots & \Psi_{3N\sigma}\Phi_{2Nu} \end{bmatrix} \mathrm{d}z. \end{cases} \tag{A.8}$$

$$\begin{cases} \mathbf{B}_{13}^w = \displaystyle\int_{-h/2}^{h/2} h_1 \begin{bmatrix} \Psi_{11}\Phi_{31} & \cdots & \Psi_{11}\Phi_{3Nu} \\ \vdots & \ddots & \vdots \\ \Psi_{1N\sigma}\Phi_{31} & \cdots & \Psi_{1N\sigma}\Phi_{3Nu} \end{bmatrix} \mathrm{d}z, & \mathbf{B}_{22}^w = \displaystyle\int_{-h/2}^{h/2} h_2 \begin{bmatrix} \Psi_{21}\Phi_{31} & \cdots & \Psi_{21}\Phi_{3Nu} \\ \vdots & \ddots & \vdots \\ \Psi_{2N\sigma}\Phi_{31} & \cdots & \Psi_{2N\sigma}\Phi_{3Nu} \end{bmatrix} \mathrm{d}z, \\ \mathbf{B}_{311}^w = \displaystyle\int_{-h/2}^{h/2} h_1 h_2 \begin{bmatrix} \Psi_{31}\Phi'_{31} & \cdots & \Psi_{31}\Phi'_{3Nu} \\ \vdots & \ddots & \vdots \\ \Psi_{3N\sigma}\Phi'_{31} & \cdots & \Psi_{3N\sigma}\Phi'_{3Nu} \end{bmatrix} \mathrm{d}z, & \mathbf{B}_{312}^w = \dfrac{1}{R_1} \displaystyle\int_{-h/2}^{h/2} F_{31} h_2 \begin{bmatrix} \Psi_{31}\Phi_{31} & \cdots & \Psi_{31}\Phi_{3Nu} \\ \vdots & \ddots & \vdots \\ \Psi_{3N\sigma}\Phi_{31} & \cdots & \Psi_{3N\sigma}\Phi_{3Nu} \end{bmatrix} \mathrm{d}z, \\ \mathbf{B}_{313}^w = \dfrac{1}{R_2} \displaystyle\int_{-h/2}^{h/2} F_{32} h_1 \begin{bmatrix} \Psi_{31}\Phi_{31} & \cdots & \Psi_{31}\Phi_{3Nu} \\ \vdots & \ddots & \vdots \\ \Psi_{3N\sigma}\Phi_{31} & \cdots & \Psi_{3N\sigma}\Phi_{3Nu} \end{bmatrix} \mathrm{d}z, \end{cases} \tag{A.9}$$

with the compliance coefficients $(E_{11}, E_{12}, E_{22}, E_{33})$ and the dimensionless coefficients (F_{31}, F_{32}, F_{33}) that correspond to $((\mathbf{C}_{345})^{-1}_{11}, (\mathbf{C}_{345})^{-1}_{12}, (\mathbf{C}_{345})^{-1}_{22}, (\mathbf{C}_{345})^{-1}_{33})$ and $(C_{13}/C_{33}, C_{23}/C_{33}, C_{36}/C_{33})$, respectively.

References

Bath, R.B., 1985. Natural frequencies of rectangular plates using characteristic orthogonal polynomials in Rayleigh–Ritz method. Journal of Sound and Vibration 102, 493–499.

Bhimaraddi, A., 1984. A higher-order theory for free vibration analysis of circular cylindrical shells. International Journal of Solids and Structures 20, 623–630.

Bhimaraddi, A., 1991. Free vibration analysis of doubly curved shallow shells on rectangular planform using three-dimensional elasticity theory. International Journal of Solids and Structures 27 (7), 897–913.

Calcote, L.R., 1969. The analysis of laminated composite structures. Van Nostrand Reinhold Company, New York.

Carrera, E., 1999a. A Reissner's mixed variational theorem applied to vibration analysis of multilayered shell. Journal of Applied Mechanics 66, 69–78.

Carrera, E., 1999b. A study of transverse normal stress effect on vibration of multilayered plates and shells. Journal of Sound and Vibration 225 (5), 803–829.

Chao, C.C., Chern, Y.C., 2000. Comparison of natural frequencies of laminates by 3-D theory, part I: rectangular plates. Journal of Sound and Vibration 230, 985–1007.

Chihara, T.S., 1978. An introduction to orthogonal polynomials. Gordon and Breach, New York.

Christensen, R.M., Zywicz, E., 1990. A three-dimensional constitutive theory for fiber composite laminated media. Journal of Applied Mechanics—ASME 57, 948–955.

Dickinson, S.M., Di Blasio, A., 1986. On the use of orthogonal polynomials in the Rayleigh–Ritz method for the study of the flexural vibration and buckling of isotropic and orthotropic rectangular plates. Journal of Sound and Vibration 108, 51–62.

Di Sciuva, M., 1987. An improved shear-deformation theory for moderately thick multilayered shells and plates. Journal of Applied Mechanics—ASME 54, 589–596.

Di Sciuva, M., Carrera, E., 1992. Elastodynamic behavior of relatively thick, symmetrically laminated, anisotropic circular cylindrical shells. Journal of Applied Mechanics 59, 222–224.

Fan, J., Zhang, J., 1992. Analytical solutions for thick, doubly curved, laminated shells. Journal of Engineering Mechanics—ASCE 118 (7), 1338–1356.

Huang, N.N., 1995. Exact analysis for three-dimensional free vibrations of cross-ply cylindrical and doubly curved laminates. Acta Mechanica 108, 23–34.

Kelly, A., Cahn, R.W., Bever, M.B., 1994. Concise Encyclopedia of composite materials. Elsevier Science, Oxford.

Kraus, H., 1967. Thin elastic shells. John Wiley and Sons, New York.

Leissa, A.W., 1973. Vibration of shells. Acoustical Society of America (NASA SP-288, Reprinted, 1993).

Leissa, A.W., Narita, Y., 1989. Vibration studies for simply supported symmetrically laminated rectangular plates. Composite Structures 12, 113–132.

Messina, A., 2001. Two generalized higher order theories in free vibration studies of multilayered plates. Journal of Sound and Vibration 242, 125–150.

Messina, A., 2002a. Free vibrations of multilayered plates based on a mixed variational approach in conjunction with global piecewise-smooth functions. Journal of Sound and Vibration 256, 103–129.

Messina, A, 2002b. A mixed variational approach and a novel C0-set of piecewise-smooth functions for an accurate two-dimensional plates theory. In: Proceedings of the 3rd International Conference on Identification in Engineering Systems, Swansea, Wales, UK.

Messina, A., Soldatos, K.P., 1999a. Influence of edge boundary conditions on the free vibrations of cross-ply laminated circular cylindrical panels. Journal of Acoustical Society of America 106, 2608–2620.

Messina, A., Soldatos, K.P., 1999b. Ritz-type dynamic analysis of cross-ply laminated circular cylinders subjected to different boundary conditions. Journal of Sound and Vibration 227, 749–768.

Messina, A., Soldatos, K.P., 2002. A general vibration model of angle-ply laminated plates that accounts for the continuity of interlaminar stresses. International Journal of Solids and Structures 39 (3), 617–635.

Philippidis, T.P., Theocaris, P.S., 1994. The transverse Poisson's ratio in fiber reinforced laminae by means of a hybrid experimental approach. Journal of Composite Materials 28, 252–261.

Reddy, J.N., 1984. Energy and variational methods in applied mechanics. John Wiley and Sons, New York.

Reddy, J.N., Liu, C.F., 1985. A higher-order shear deformation theory of laminated elastic shells. International Journal of Engineering Science 23 (3), 319–330.

Reissner, E., 1986. On a mixed variational theorem and on shear deformable plate theory. International Journal for numerical methods in engineering 23, 193–198.

Roy, A.K., Tsai, S.W., 1992. Three-dimensional effective moduli of orthotropic and symmetric laminates. Journal of Applied Mechanics 59, 39–47.

Sansone, G., 1959. In: Courant, R., Bers, L., Stoker, J.J. (Eds.), Orthogonal Functions, vol. IX. Interscience Publishers, London (English edition translated from the Italian by A. Diamond, E. Hille).

Soldatos, K.P., 1994. Review of three dimensional dynamic analyses of circular cylinders and cylindrical shells. Applied Mechanics Reviews 47 (10), 501–516.

Soldatos, K.P., Timarci, T., 1993. A unified formulation of laminated composite, shear deformable, five degrees-of-freedom cylindrical shell theories. Composite Structures 25, 165–171.

Timarci, T., Soldatos, K.P., 1995. Comparative dynamic studies for symmetric cross-ply circular cylindrical shells on the basis of a unified shear deformable shell theory. Journal of Sound and Vibration 187 (4), 609–624.

Tsai, S.W., Hahn, H.T., 1980. Introduction to composite materials. Technomic, Lancaster.

Vinson, J.R., Sierakowski, R.L., 2002. The behavior of structures composed of composite materials. Kluwer Publishers, London.

Whitney, J.W., 1987. Structural analysis of laminated anisotropic plates. Technomic, Lancaster.

Wu, C.P., Tarn, J.Q., Chi, S.M., 1996. An asymptotic theory for dynamic response of doubly curved laminated shells. International Journal of Solids and Structures 33 (26), 3813–3841.

Xavier, P.B., Chew, C.H., Lee, K.H., 1995. Buckling and vibration of multilayer orthotropic composite shells using a simple higher-order layerwise theory. International Journal of Solids and Structures 32 (23), 3479–3497.

Ye, J., Soldatos, K.P., 1994. Three-dimensional vibration of laminated cylinders and cylindrical panels with symmetric or antisymmetric cross-ply lay-up. Composites Engineering 4 (4), 429–444.

Yuan, F.G., Hsieh, C.C., 1998. Three-dimensional wave propagation in composite cylindrical shells. Composite Structures 42, 153–167.